Journal of Catalysis **208,** 435–447 (2002)
doi:10.1006/jcat.2002.3596

An Investigation of Promoter Effects in the Reduction of NO by H_2 under Lean-Burn Conditions

R. Burch[1] and M. D. Coleman

School of Chemistry, Queen's University Belfast, David Keir Building, Stranmillis Road, Belfast, BT9 5AG, N. Ireland

Received December 12, 2001; revised February 15, 2002; accepted February 15, 2002

The reduction of NO by H_2 has been investigated under lean conditions at temperatures representative of automotive "cold-start" conditions (<200°C) using MoO_3- and Na_2O-modified Pt/Al_2O_3 and Pt/SiO_2 catalysts. It has been found that small additions of sodium significantly increase the NO conversion while larger loadings of sodium have a severe poisoning effect. However, in the presence of excess O_2 no enhancement in nitrogen selectivity at low temperatures has been observed for all loadings of Na. Indeed, an adverse effect has been found at higher temperatures. Addition of molybdenum as a promoter results in increases in NO conversion and nitrogen selectivity for all loadings tested. The optimal formulation was determined to be 1% Pt/10% MoO_3/0.27% Na_2O/Al_2O_3. Steady-state isotopic-transient kinetic (SSITK) experiments were performed on this and a "model" $Pt/MoO_3/Na_2O/SiO_2$ catalyst using labelled nitric oxide in order to estimate the surface concentrations of species leading to N_2, N_2O, and retained NO. The data reveal significantly greater surface concentrations of N_2 precursors over the modified catalysts for both the Pt/Al_2O_3 and Pt/SiO_2 systems and this has been used to rationalise the increased selectivity to N_2. An additional significant effect of the molybdenum promoter has been proposed because when the concentrations of N_2 intermediates and the amount of available platinum in the modified catalysts are calculated, the "storage" of N_2 precursors on the MoO_3 seems to occur. This effect has been further explored using the modified SiO_2 catalyst in non-steady-state transient experiments where the reductant supply (i.e., the H_2) is cut off. It has been found that the decay in the production of N_2 is very significantly delayed in comparison with the unmodified catalysts, and it is proposed that this is consistent with the trapping on the Mo of a *reduced* intermediate that can form N_2 even in the absence of the normal H_2 reductant. The mechanistic consequences of these novel results are discussed.

Key Words: **SSITKA; NO/H_2; lean burn; platinum; molybdenum promoter.**

INTRODUCTION

The adverse health and environmental effects caused through NO_x (defined as $NO+NO_2$) release from both mobile and stationary sources are well-known (1–3) and has resulted in increasingly stringent legislation (4). Whilst three-way catalysts (TWCs) have been successfully used for several decades with engines that operate close to stoichiometric the current technology cannot remove NO_x at low temperatures or under lean conditions (5–7). As a result, there is a need to find catalytic systems able to operate under these conditions (8). To this end there has been much interest in using the hydrocarbons present either in the on-board fuel or in the exhaust itself to carry out the reduction.

A variety of hydrocarbons, ranging from methane (9–13), ethene (14–16), and propane/-ene (17–22) to larger molecules (23–27), have been shown to selectively react with NO_x in the presence of excess oxygen but the lack of any significant activity below ~200°C remains a serious problem. Ammonia is a possible alternative and is often used as the reductant in stationary power sources (28). However, due to ammonia slip and the lack of a distribution network it is still desirable to find a way to remove NO_x using the normal on-board fuel.

Hydrogen may offer a solution to these problems since it can be generated on-board from the fuel and is active at low temperatures. The NO/H_2 reaction has been well investigated over the past few decades (29–34). In the 1970s Kobylinski and Taylor screened a number of supported noble metals for activity and found both palladium and platinum to be particularly active (35). Furthermore, they also reported that N_2 and NH_3 were the main reduction products. More recently, both Harkness and Lambert, and Marina *et al.* have reported that sodium can be used to increase NO conversion and N_2 selectivity over platinum-based catalysts (36, 37). These authors proposed that these observations could be explained by considering that since sodium is electropositive the chemisorption strength of an electron acceptor adsorbate (i.e., NO) would be increased. It was further surmised that the increased strength of the Pt–NO interaction caused a weakening of the N–O bond, leading to increased dissociation. Sodium addition has also been found to promote reaction characteristics over catalysts based on platinum, palladium, and rhodium using both CO and hydrocarbon reductants (38–47). However, when using methane as a reductant sodium addition has been

[1] To whom correspondence should be addressed.

0021-9517/02 $35.00

found to poison the activity of a palladium catalyst (48). In this case it was proposed that since methane is a weaker adsorbate than NO (in contrast to the NO/propene system), promoting the adsorption of NO by using sodium is undesirable since it results in oxygen poisoning of the catalyst. Halasz *et al.* have reported the promotion of PdO/Al_2O_3 with MoO_3 (49, 50). However, while the activity towards the NO/H_2 reaction was found to increase as a consequence of this modification, no effect was observed under lean-burn conditions (51).

With regard to investigations of the NO/H_2 reaction in an excess of oxygen there is a relative dearth of literature (52–55). In a previous paper we demonstrated that hydrogen could be used to selectively reduce NO under lean-burn conditions over platinum-based catalysts (56). However, in common with many such systems using a hydrocarbon reductant (57) it was found that significant amounts of undesirable N_2O were produced in addition to N_2 (no NH_3 was seen). Tanaka *et al.* have modified Pt/SiO_2 with molybdenum and sodium oxide promoters, and for the reduction of NO with C_3H_6, H_2, and CO they have found increases in the nitrogen selectivity (58–60). They rationalised the results on the basis that the enhanced selectivity was due to the suppression of the oxidation of the platinum under lean conditions.

In this paper we present the results of a kinetic investigation into the activity and nitrogen selectivity of modified Pt/Al_2O_3 catalysts as a function of MoO_3 and Na_2O loadings using H_2 as the reductant under lean-burn conditions in relation to cold-start or low-temperature operation. On the basis of steady-state isotopic-transient kinetic analysis (SSITKA) (61) for an optimised $Pt/MoO_3/Na_2O/Al_2O_3$ and a "model" $Pt/MoO_3/Na_2O/SiO_2$ catalyst, we provide a rationalisation for the mode of operation of these oxide promoters.

EXPERIMENTAL

Catalyst Preparation

Supported Pt catalysts (nominal composition, 1 wt%) were prepared by incipient wetness using aqueous solutions of dinitrodiamine platinum(II) with acid-washed silica (Grace 432) or alumina (Akzo CK300, supplied by Criterion) that had been precalcined overnight at 500 and 700°C, respectively. The prepared catalysts were dried at 120°C overnight and then calcined at 500°C for 2 h. In addition, the oxide supports were modified by addition of MoO_3 (using ammonium heptamolybdate) and/or Na_2O (using sodium acetate) promoters, and also by incipient wetness, except in the case of very high MoO_3 loadings where the solubility limit of the ammonium heptamolybdate required excess solution to be used. After drying overnight at 120°C and calcinations for 2 h at 500°C, the Pt was added as before. For convenience, the catalysts are labelled as follows: e.g., 1% Pt/10% MoO_3/0.27% Na_2O/Al_2O_3 is written as Pt/10Mo/0.27Na.

Characterisation

BET surface areas were measured using a Micromeritics ASAP 2010 system. The SiO_2 had a surface area of 283 $m^2\ g^{-1}$ and the Al_2O_3 had a surface area of 180 $m^2\ g^{-1}$. Pt surface areas were determined using pulses of H_2 in a Micromeritics AutoChem 2910 system—details are given under the Results section.

Kinetic Measurements

The catalysts (typically 100 mg) were loaded into a quartz reactor and held in place with quartz wool plugs. A thermocouple was located in the centre of the catalyst bed and the reactor was connected to a stainless steel gas handling system fitted with Area mass flow controllers for the production of the various gaseous reaction mixtures. Using He as the makeup gas, the total flow rate was set at 200 $cm^3\ min^{-1}$, corresponding to 120,000 $cm^3\ g^{-1}\ h^{-1}$. The effluent from the reactor was analysed by an online gas chromatograph (Perkin–Elmer Autosystem XL, with Nelson software) fitted with Heysep-n and 13× molecular sieve columns, and by a Signal chemiluminscence NO_x analyser. The large excess of O_2 made separate analysis of N_2 problematical so, in general, this was determined by difference since mass spectrometric analysis had shown that NH_3 was not formed under lean conditions:

$$[N_2] = \frac{[NO_x \text{ in feed}] - ([NO_x \text{ in effluent}] + 2[N_2O \text{ in effluent}])}{2}.$$

The percentage NO conversion was calculated from

$$NO_{conv} = \frac{[NO \text{ in feed}] - [NO \text{ in effluent}]}{[NO \text{ in feed}]} \times 100.$$

The percentage N_2 selectivity was calculated from

$$S_{N_2} = \frac{[N_2 \text{ in effluent}]}{[N_2 \text{ in effluent}] + [N_2O \text{ in effluent}]} \times 100.$$

Transient kinetic studies, both using simple gas-switching techniques and steady-state isotopic-transient kinetic (SSITK) methods, were undertaken using a specially designed, very low dead-volume apparatus with accurate control of pressures (monitored by high-precision WIKA transducers) on either side of a fast-switching valve (Valco). Prior to a switch, whether using isotopically labelled gases or not, the flows and pressures were carefully balanced so that when the switch was made there would be no upset to the gas flow that could lead to erroneous readings on the mass spectrometer (VG Gaslab 300 Mass Spectrometer).

RESULTS

Steady-State Experiments

The surface areas of the Pt in the various catalysts, as measured using the H_2 pulse method, are given in Table 1. For the alumina-supported catalysts, addition of Na appears initially to increase the exposed Pt surface area, but at higher loading the uptake of H_2 is significantly suppressed. Addition of Mo oxide has a clear effect and severely reduces the amount of H_2 chemisorbed. Surprisingly, with the silica-supported catalyst even the addition of a very large amount of Mo oxide has no significant effect on the H_2 chemisorption. The calculated Pt dispersion ranges from 54 to 2.2%, although it must be understood that partial coverage of the Pt particles by Na and/or Mo oxide could reduce the amount of H_2 chemisorbed and cause the Pt dispersion to appear to decrease.

The NO conversion as a function of temperature for the Pt/Al_2O_3 and Na-modified catalysts is shown in Fig. 1. The base catalyst has a good activity for the reduction of NO under these lean-burn conditions with a conversion peak of 75% at 125°C. Addition of the smallest amount of Na (0.27%) results in a significant increase in the level of NO reduction with a peak now at almost 90% conversion and a much improved performance on the higher temperature side of the maximum. However, further increases in the Na loading first result in a loss of activity at the lower temperatures and then in a dramatic loss of activity at all temperatures when the Na content is increased to 5 and then 10%. Even allowing for the loss of Pt area, as measured by H_2 chemisorption (see Table 1), there is a clear loss of activity when high loadings of Na are used.

The H_2 conversion (results not shown) corresponding to the NO reduction profiles shown in Fig. 1 reflects the activity of the catalysts. Thus, as the Na loading is increased, the temperature for 20% conversion of H_2 varies as follows: Pt (100°C), Pt/0.27Na (100°C), Pt/1Na (140°C), Pt/5Na (150°C), and Pt/10Na (>190°C), which comparison with Fig. 1 shows is close to the temperature at which the NO reduction lights off.

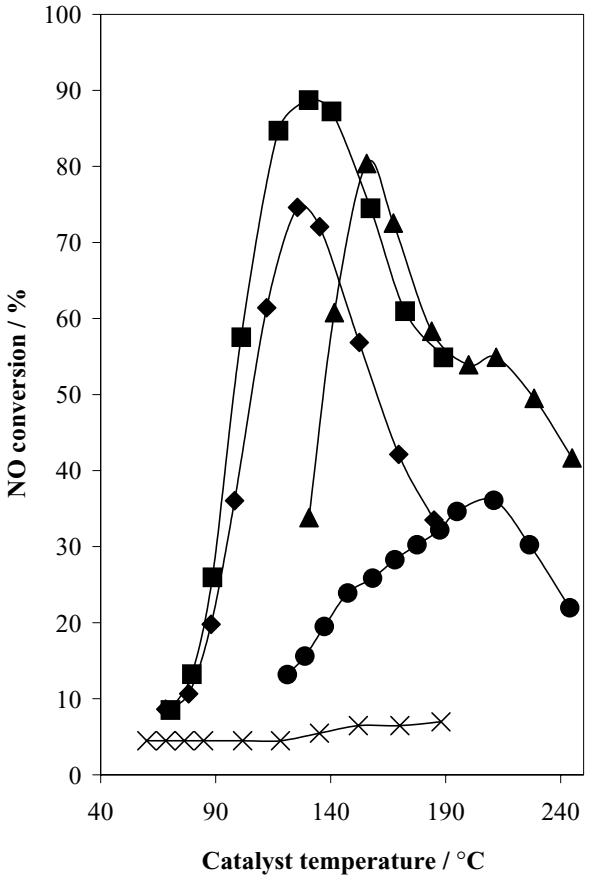

FIG. 1. NO conversion as a function of temperature for various sodium-modified catalysts. ◆, Pt/Al_2O_3; ■, $Pt/0.27Na/Al_2O_3$; ▲, $Pt/1Na/Al_2O_3$; ●, $Pt/5Na/Al_2O_3$; ×, $Pt/10Na/Al_2O_3$. Reaction conditions: 1000 ppm NO, 4000 ppm H_2, 6% O_2, 200 cm^3 min^{-1} total flow, 100 mg of catalyst.

TABLE 1

Pt Surface Areas as Determined Using the H_2 Pulse Method

Catalyst	H_2 uptake (μmol g^{-1})	Pt surface area (m^2 g^{-1})	Pt dispersion (%)
Pt/Al_2O_3	10.8	1.04	42.0
$Pt/0.27Na/Al_2O_3$	13.9	1.34	54.2
$Pt/1Na/Al_2O_3$	13.5	1.30	52.8
$Pt/5Na/Al_2O_3$	9.60	0.93	37.5
$Pt/10Na/Al_2O_3$	4.73	0.46	18.4
$Pt/2.5Mo/0.27Na/Al_2O_3$	7.81	0.75	30.4
$Pt/10Mo/0.27Na/Al_2O_3$	3.26	0.32	12.7
$Pt/23Mo/0.27Na/Al_2O_3$	4.78	0.46	18.7
$Pt/46Mo/0.27Na/Al_2O_3$	0.54	0.05	2.2
Pt/SiO_2	5.31	0.51	20.7
$Pt/46Mo/0.27Na/SiO_2$	5.13	0.50	20.1

In the reduction of NO, the selectivity to N_2 rather than N_2O is important since N_2O is itself a pollutant. It has been shown that under stoichiometric (or rich) conditions the addition of sodium can markedly increase the selectivity to N_2 rather than to N_2O (36–47). However, Fig. 2 shows that under lean-burn conditions there is no change in the selectivity in the temperature range from 90 to 140°C. Indeed, at higher temperatures, the selectivity to N_2 is actually decreased somewhat when sodium is added. Clearly, there are differences in the performance of our catalysts under lean-burn conditions and those reported in the literature tested under stoichiometric conditions.

Figure 1 has shown that the optimum effect of sodium on activity under our lean-burn conditions is found with the addition of only 0.27% Na. Therefore, this was selected as the reference material in order to examine the effect of adding molybdenum. Figure 3 shows that addition of molybdenum has a significant effect on the activity for NO reduction.

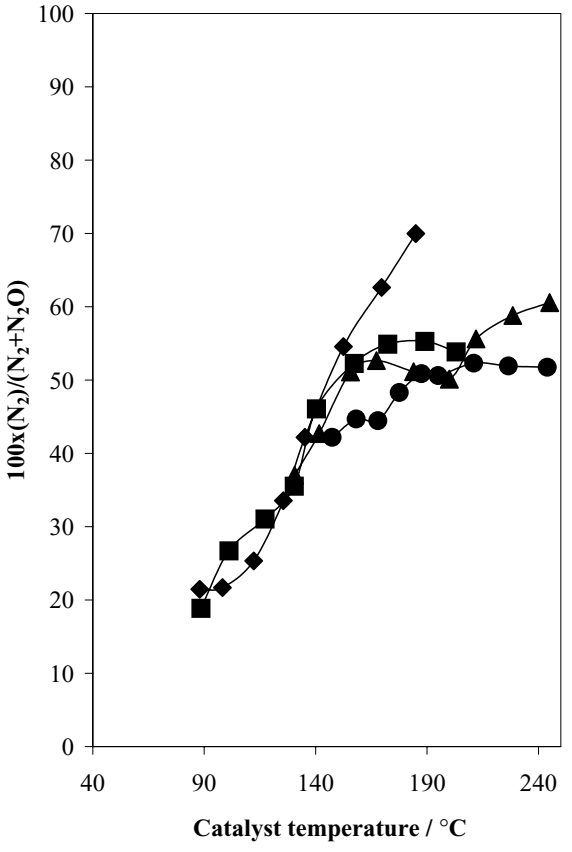

FIG. 2. N_2 selectivity as a function of temperature for various sodium-modified catalysts. ◆, Pt/Al_2O_3; ■, $Pt/0.27Na/Al_2O_3$; ▲, $Pt/1Na/Al_2O_3$; ●, $Pt/5Na/Al_2O_3$. Reaction conditions: 1000 ppm NO, 4000 ppm H_2, 6% O_2, 200 cm^3 min^{-1} total flow, 100 mg of catalyst.

In all cases, the performance at lower temperatures is enhanced, and in the specific cases where 2.5 or 10% MoO_3 has been added, the conversion of NO exhibits a maximum that exceeds 90%. The 10% MoO_3 catalyst also shows improved performance at the higher temperatures where the conversion stays above 70%, up to at least 180°C. The conversion of H_2 (results not shown) parallels the NO reduction profiles, with the more active catalysts lighting off some 20–30°C lower than for the unpromoted Pt catalyst.

The product selectivity with these Mo-promoted catalysts is shown in Fig. 4. In this case, there is a significant improvement in the selectivity to N_2 rather than to N_2O. For the most active catalysts, the selectivity to N_2 has increased by around 30% in the middle range of temperatures. In order to try to understand the reason for the improved selectivity of the molybdenum-promoted catalysts under lean-burn conditions, we have performed a comprehensive set of transient kinetic experiments that are now described.

Transient Kinetic Experiments on Alumina-Supported Catalysts under Rich Conditions

In order to further probe the nature of the changes induced in the Pt catalysts by the addition of sodium and/or molybdenum to the alumina-supported Pt catalyst, we first investigated the NO/H_2 reaction *in the absence of oxygen*. One reason is that under oxidising conditions the alumina support has a high affinity for adsorbing NO_2 as a surface nitrate and this completely masks any transient isotope effects that might be occurring on the metal. Therefore, we tried to circumvent this problem (see later) by first confirming that the promoted alumina-supported catalysts do indeed show differences even under oxygen-free conditions, and then by investigating a model silica-supported catalyst that does not have this NO_2 adsorption problem.

Figure 5 shows the transient curves for the isotopic switching experiment, in which ^{14}NO is replaced at steady state with ^{15}NO, using the Pt/Al_2O_3 catalyst at 70°C. The $^{14}N^{15}NO$ profile shows a small maximum (masked by other profiles on figure) a very short time after the switch and then declines rapidly to zero, indicating that the formation of this mixed isotope product requires the presence of gaseous NO. Similarly, the $^{15}N_2O$ profile rises rapidly to a constant value, indicating that N_2O precursors have a short lifetime on the catalyst surface prior to desorption. On the other hand, the

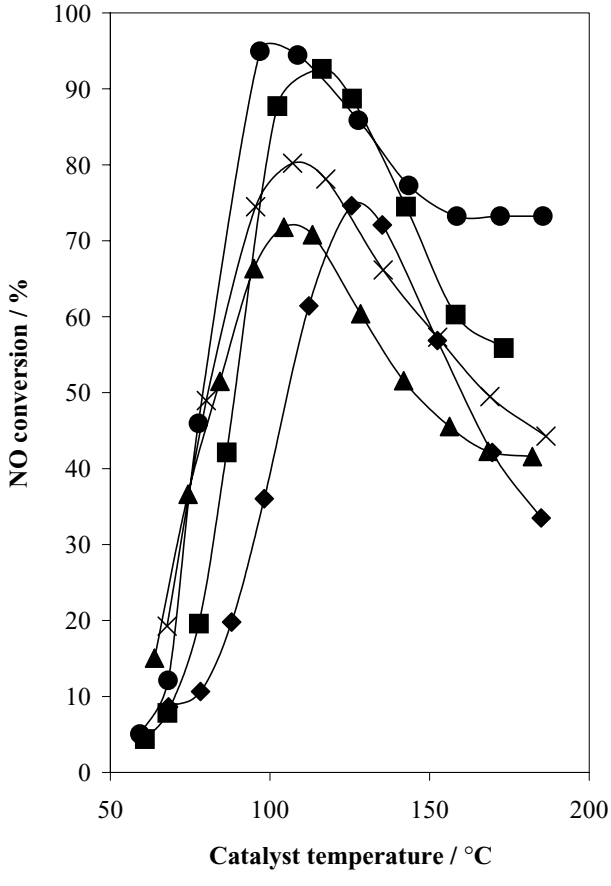

FIG. 3. NO conversion as a function of temperature for various sodium- and molybdenum-modified catalysts. ◆, Pt/Al_2O_3; ■, $Pt/2.5Mo/0.27Na/Al_2O_3$; ●, $Pt/10Mo/0.27Na/Al_2O_3$; ▲, $Pt/23Mo/0.27Na/Al_2O_3$; ×, $Pt/46Mo/0.27Na/Al_2O_3$. Reaction conditions: 1000 ppm NO, 4000 ppm H_2, 6% O_2, 200 cm^3 min^{-1} total flow, 100 mg of catalyst.

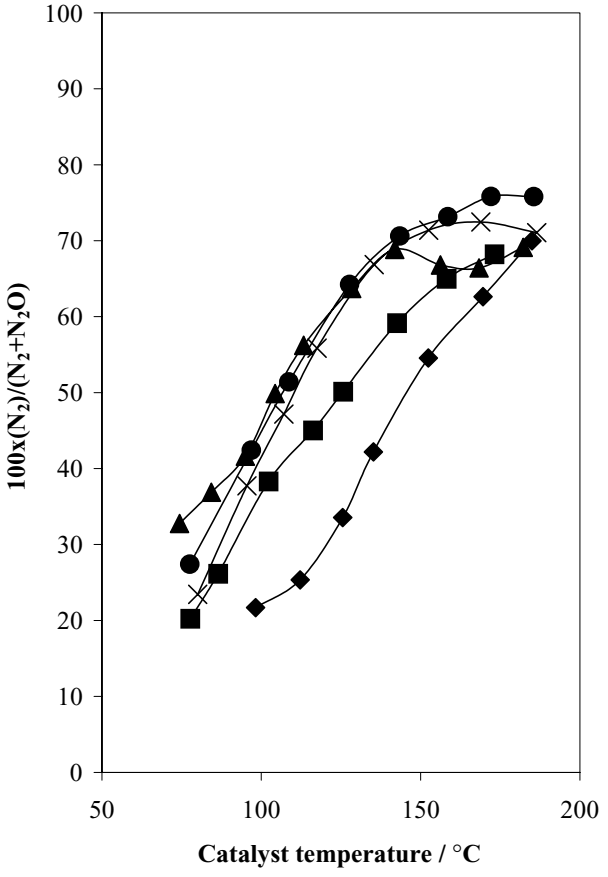

FIG. 4. N_2 selectivity as a function of temperature for various sodium- and molybdenum-modified catalysts. ◆, Pt/Al_2O_3; ■, $Pt/2.5Mo/0.27Na/Al_2O_3$; ●, $Pt/10Mo/0.27Na/Al_2O_3$; ▲, $Pt/23Mo/0.27Na/Al_2O_3$; ×, $Pt/46Mo/0.27Na/Al_2O_3$. Reaction conditions: 1000 ppm NO, 4000 ppm H_2, 6% O_2, 200 cm^3 min^{-1} total flow, 100 mg of catalyst.

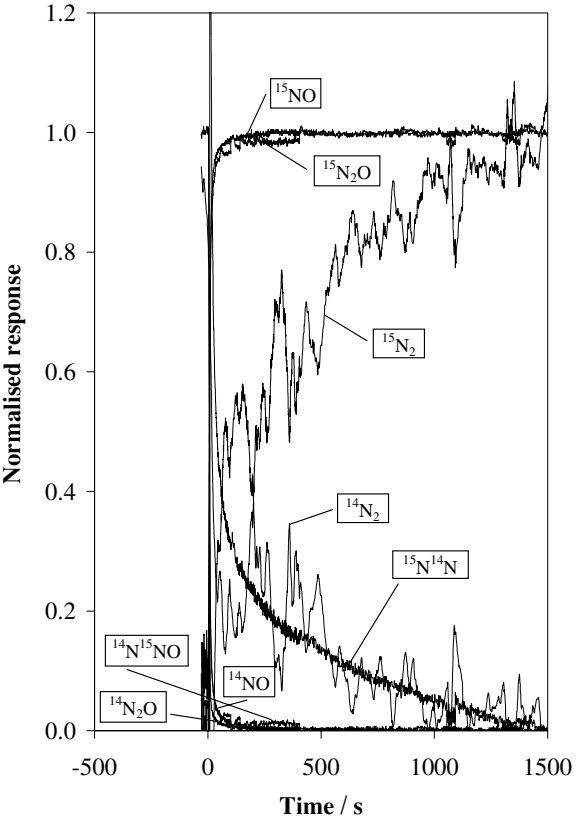

FIG. 5. Concentration profiles as a function of time after a SSITK switch of ^{15}NO for ^{14}NO for a Pt/Al_2O_3 catalyst. Switch from (0.76% ^{14}NO/Ar/1.08% H_2) to (0.76% ^{15}NO/He/1.08% H_2) at 70°C for 100 mg of catalyst at a total gas flow rate of 100 cm^3 min^{-1}.

$^{14}N_2$ profile decays slowly to zero over a period of about 1500 s, as also does the $^{14}N^{15}N$ profile, indicating that these products are formed from ^{14}N that is retained on the catalyst surface for a long period of time.

Figure 6 shows the corresponding results for the sodium-modified catalyst (Pt/0.27Na). The results mainly differ in the nitrous oxide profiles. In this case, both the $^{14}N^{15}NO$ and the $^{14}N_2O$ curves take longer to decay, and this seems to parallel the slower displacement of ^{14}NO from the system (compare Figs. 5 and 6, and see also the quantitative data later in Table 2). On the other hand, the profiles for $^{14}N_2$ and $^{14}N^{15}N$ are rather similar for both the Pt and the Pt/0.27Na catalysts.

Much more significant differences in the profiles are seen in Fig. 7 for the Pt/10Mo catalyst. In this case the $^{14}N^{15}NO$ and the $^{14}N_2O$ curves decay significantly faster than the NO curve whereas the $^{14}N^{15}N$ curve shows a peak maximum at a later time than before and, moreover, does not even decay to zero even after 1500 s. Figure 8 shows that for the doubly promoted Pt/10Mo/0.27Na catalyst these effects are further enhanced, with the NO retention being longer and the $^{14}N^{15}N$ decay being slower again.

Using standard SSITK curve analysis procedures (61) we estimated the concentration of intermediates on the surface of each catalyst that leads to the different nitrogen-containing products. These are summarised in Table 2. It

TABLE 2

Concentrations of Adsorbed Species (μmol g^{-1}) Leading to N_2 and N_2O Products and to NO Desorption as Estimated by Analysis of the SSITK Profiles Shown in Figs. 5–12

Catalyst	$C(N_2)$	$C(N_2O)$	C(NO)	ΣC
Pt/Al_2O_3	15.0 ± 0.2	8.3 ± 0.5	27.4 ± 4.1	50.7 ± 4.8
$Pt/0.27Na/Al_2O_3$	17.4 ± 0.3	17.2 ± 0.8	75.1 ± 3.6	109.7 ± 4.7
$Pt/10Mo/Al_2O_3$	34.4 ± 6.9	3.4 ± 0.6	63.8 ± 3.8	101.6 ± 11.3
$Pt/10Mo/0.27Na/Al_2O_3$	56.0 ± 9.3	3.2 ± 0.6	95.7 ± 3.8	154.9 ± 13.7
Pt/SiO_2	3.6 ± 0.2	3.5 ± 0.5	4.9 ± 4.2	12.0 ± 4.9
$Pt/46Mo/0.27Na/SiO_2$	126.3 ± 1.5	1.6 ± 0.6	19.9 ± 3.8	147.8 ± 5.9
Pt/SiO_2 (lean conditions)	10.9 ± 2.2	1.5 ± 1.1	18.1 ± 2.3	30.5 ± 5.6
$Pt/46Mo/0.27Na/SiO_2$ (lean conditions)	57.1 ± 10.0	1.8 ± 1.4	14.2 ± 1.6	73.1 ± 13.0

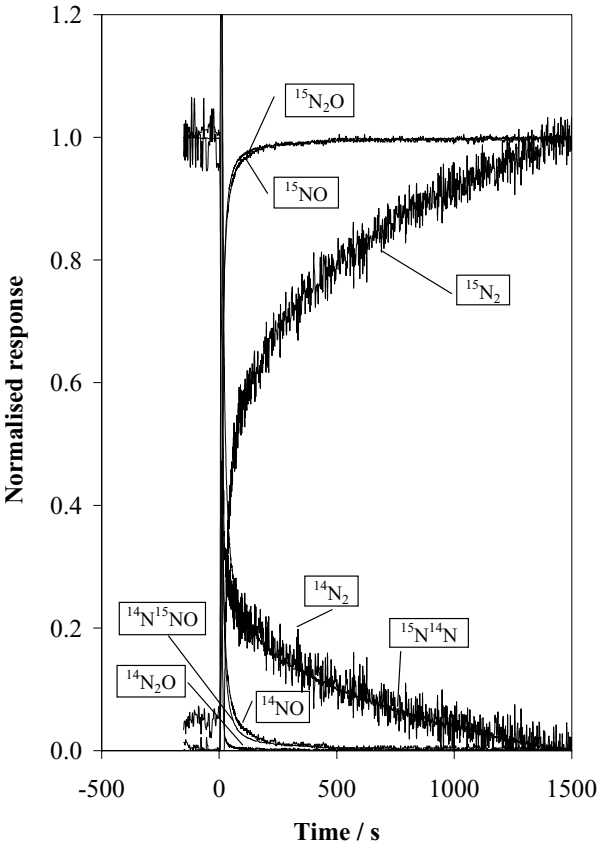

FIG. 6. Concentration profiles as a function of time after a SSITK switch of ^{15}NO for ^{14}NO for a $Pt/0.27Na/Al_2O_3$ catalyst. Switch from (0.76% ^{14}NO/Ar/1.08% H_2) to (0.76% ^{15}NO/He/1.08% H_2) at 70°C for 100 mg of catalyst at a total gas flow rate of 100 cm^3 min^{-1}.

is clear that addition of sodium has a small positive effect on the concentration of N_2 precursors and a large positive effect both on the concentration of N_2O precursors and on the retention of NO. Addition of molybdenum, on the other hand, increases markedly the concentration of N_2 precursors and the retention of NO but decreases sharply the concentration of N_2O precursors. When both molybdenum and sodium are added, there is a further sharp rise in the concentration of N_2 precursors and in the NO retention but hardly any further change in the already small value for the concentration of N_2O precursors.

Transient Kinetic Experiments on Silica-Supported Catalysts under Rich Conditions

As indicated earlier, all our attempts to perform transient kinetic experiments using ^{15}NO with alumina-supported catalysts under lean-burn conditions have been unsuccessful because the exchange of ^{15}N with $^{14}NO_x$ species adsorbed on the alumina support completely mask any transient changes due to the Pt at the temperatures of our experiments. Therefore, in order to further probe the details of the promoting effect of sodium and/or molybdenum we have prepared a "model" silica-supported catalyst using a high loading of molybdenum so as to amplify any effects that might be occurring.

Figure 9 shows first the effect of switching ^{15}NO for ^{14}NO with the Pt/SiO_2 catalyst in the absence of oxygen. Comparison with Fig. 5 illustrates the complication of using alumina as a support. Thus, with silica, which does not adsorb NO, Fig. 9 shows that the $^{14}N_2$ profile (see magnified portion of Fig. 9) decays to zero very rapidly after the switch is made. Similarly, the $^{14}N^{15}N$ mixed isotope decays to zero much more rapidly with the silica-supported catalyst.

Repeating this switching experiment in the absence of oxygen with the $Pt/46Mo/0.27Na/SiO_2$ catalyst gives the results shown in Fig. 10. The most important point to note is the very slow decay in the $^{14}N^{15}N$ profile. Even after 600 s this still gives a signal corresponding to about 50% of the initial value. The corresponding estimated values for the concentration of N_2 and N_2O precursors on the surface, and the amount of retained NO, for these two silica-supported catalysts are given in Table 2. These results show that

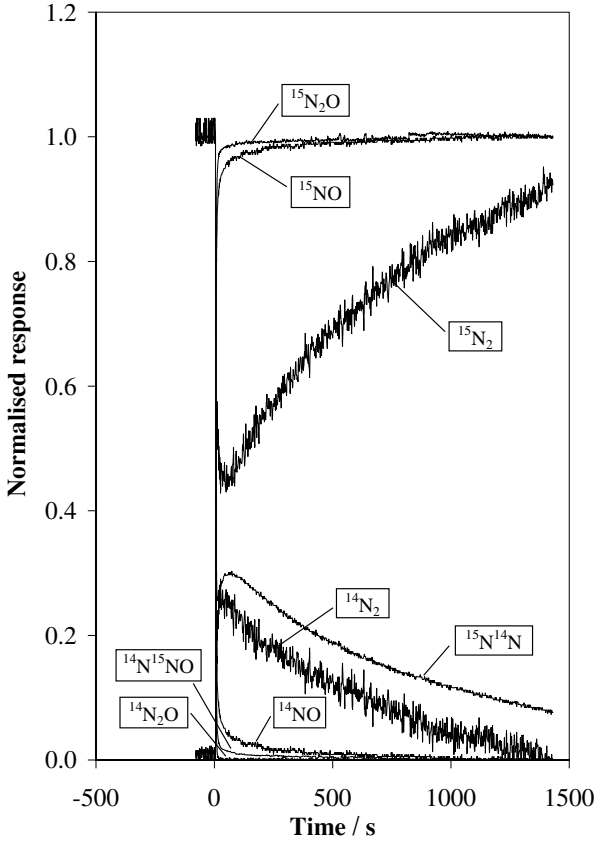

FIG. 7. Concentration profiles as a function of time after a SSITK switch of ^{15}NO for ^{14}NO for a $Pt/10Mo/Al_2O_3$ catalyst. Switch from (0.76% ^{14}NO/Ar/1.08% H_2) to (0.76% ^{15}NO/He/1.08% H_2) at 70°C for 100 mg of catalyst at a total gas flow rate of 100 cm^3 min^{-1}.

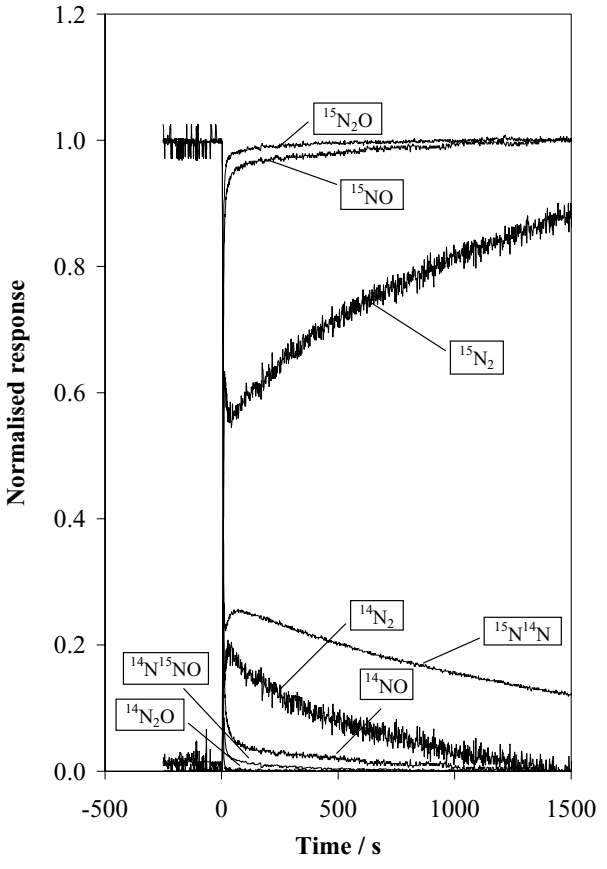

FIG. 8. Concentration profiles as a function of time after a SSITK switch of ^{15}NO for ^{14}NO for a Pt/10Mo/0.27Na/Al_2O_3 catalyst. Switch from (0.76% ^{14}NO/Ar/1.08% H_2) to (0.76% ^{15}NO/He/1.08% H_2) at 70°C for 100 mg of catalyst at a total gas flow rate of 100 cm^3 min^{-1}.

addition of the promoters has a major effect in increasing the concentration of N_2 precursors, a significant effect on increasing the amount of NO retained, and a very small negative effect on the concentration of N_2O precursors.

An important distinction between the alumina- and the silica-supported catalysts is that in the case of the alumina-supported catalysts the $^{14}N_2$ peak decays quite slowly whereas in the silica-supported case the decay is very fast. This seems to suggest, from the silica-supported catalyst results, that the formation of N_2 requires *gaseous* NO, in line with conclusions drawn from previous related work from our laboratory (33, 34, 55).

Transient Kinetic Experiments on Silica-Supported Catalysts under Lean Conditions

Figure 11 shows the results of switching ^{15}NO for ^{14}NO under lean conditions (6% O_2). The $^{14}N^{15}NO$ decays more rapidly than the NO, which, comparison with Fig. 9 shows, is significantly delayed under lean conditions. Moreover, the decay of the $^{14}N^{15}N$ profile is much faster in the presence of excess oxygen (ca. 200 as compared with >600 s after the switch). Figure 12 shows the corresponding results for the promoted silica-supported catalyst. In this case it is notable that the $^{14}N^{15}NO$ profile decays very fast. On the other hand, the $^{14}N^{15}N$ curve decays much more slowly in the case of the promoted catalyst. This trend parallels that shown earlier for the switching experiments on the same catalysts under rich conditions. Consequently, it seems reasonable to assume that similar mechanisms are involved in both cases.

Using the standard SSITK peak profile analysis we arrive at the concentrations of N_2 and N_2O precursors and the amount of retained NO shown in Table 2. Addition of the promoters results in a large increase in the concentration of N_2 precursors but, within experimental error, essentially no change in the concentration of N_2O precursors or the amount of retained NO.

Non-Steady-State Transient Experiments on Silica-Supported Catalysts under Lean Conditions

The SSITK experiments have shown that promotion of the Pt/SiO_2 catalyst results in significant differences in

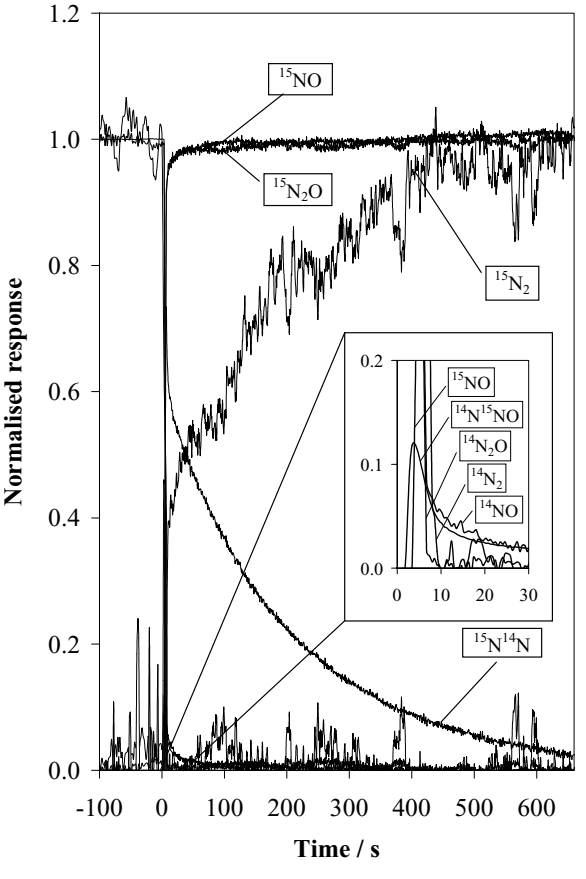

FIG. 9. Concentration profiles as a function of time after a SSITK switch of ^{15}NO for ^{14}NO for a Pt/SiO_2 catalyst. Switch from (0.76% ^{14}NO/Ar/1.08% H_2) to (0.76% ^{15}NO/He/1.08% H_2) at 55°C for 100 mg of catalyst at a total gas flow rate of 100 cm^3 min^{-1}.

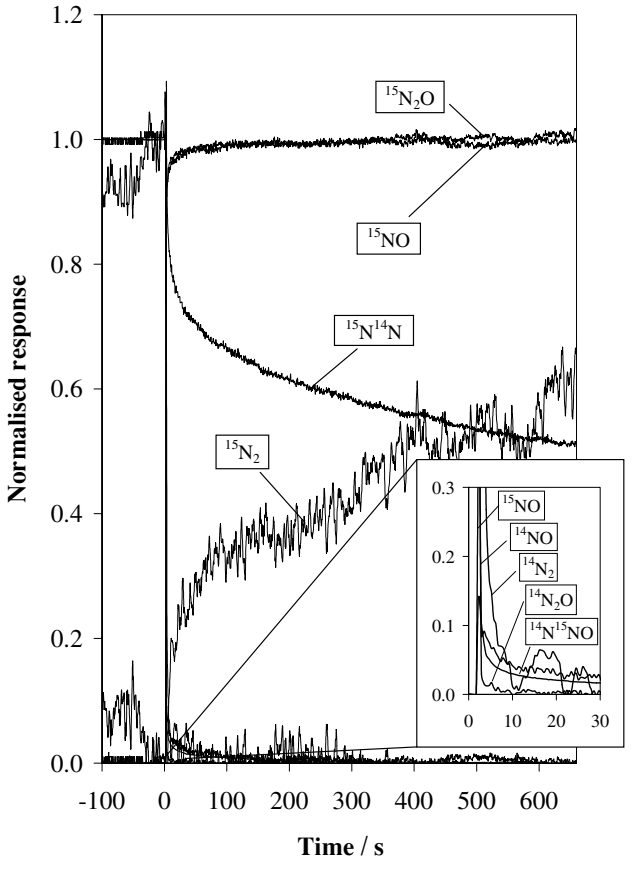

FIG. 10. Concentration profiles as a function of time after a SSITK switch of ^{15}NO for ^{14}NO for a Pt/46Mo/0.27Na/SiO_2 catalyst. Switch from (0.76% ^{14}NO/Ar/1.08% H_2) to (0.76% ^{15}NO/He/1.08% H_2) at 80°C for 100 mg of catalyst at a total gas flow rate of 100 cm^3 min^{-1}.

the concentrations of surface intermediates, leading to the various reduced products. As a further probe of these materials, we performed switching experiments in which the H_2 was cut off completely. To further increase the sensitivity of the switching experiments, we used high concentrations of both O_2 and H_2 so that the conditions were still lean. Figure 13 shows the results with the Pt/SiO_2 catalyst. As soon as the H_2 was switched off the concentration of N_2O immediately dropped to zero. Conversely, the N_2 profile showed an initial sharp, but short-lived, increase in concentration before decaying to zero after ca. 75 s. This much greater formation of N_2 compared to N_2O is consistent with the SSITKA data summarised for this catalyst in Table 2. In parallel with the decreasing concentration of N_2 is an increase in the concentration of NO_2, indicating, as expected, that the Pt surface changes from a reduced to an oxidised state when the H_2 is removed.

Figure 14 shows the remarkable difference observed for the promoted Pt catalysts when the hydrogen supply is cut off. In this case, while the N_2O still falls rapidly to zero, the N_2 concentration rises to a very high value and only decays to zero after about 150 s. Moreover, the increase in the concentration of NO_2 now also takes a similar length of time, again suggesting that the Pt surface changes from a reduced to an oxidised state after the hydrogen is removed. However, in this case, both the very large amount of N_2 formed and the long time before the Pt becomes oxidised suggest that in the promoted catalyst there is a source of a reductant that can continue to convert NO to N_2 in the absence of H_2. Comparison between the unpromoted Pt/SiO_2 catalyst and the promoted catalyst suggests that this additional reductant may be associated with the promoters. Since the main promoter is molybdenum, it further seems reasonable to associate the additional reductant with the molybdenum oxide.

Finally, Figs. 15 and 16 show the reverse experiments, in which the H_2 is added to the NO/O_2 mixture. It is important to note that the rise in the concentration of H_2O and the fall in the concentration of NO_2 are very similar in both cases, suggesting that the reduction of the catalysts occurs on the same time scale in both cases. However, very marked differences are observed between the two catalysts.

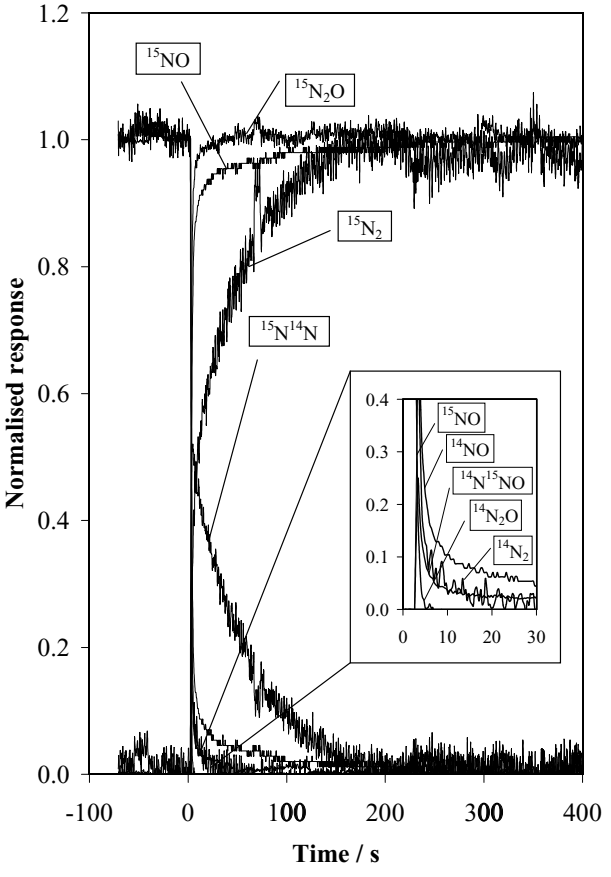

FIG. 11. Concentration profiles as a function of time after a SSITK switch of ^{15}NO for ^{14}NO for a Pt/SiO_2 catalyst. Switch from (0.76% ^{14}NO/Ar/1.08% H_2/6% O_2) to (0.76% ^{15}NO/He/1.08% H_2/6% O_2) at 105°C for 100 mg of catalyst at a total gas flow rate of 100 cm^3 min^{-1}.

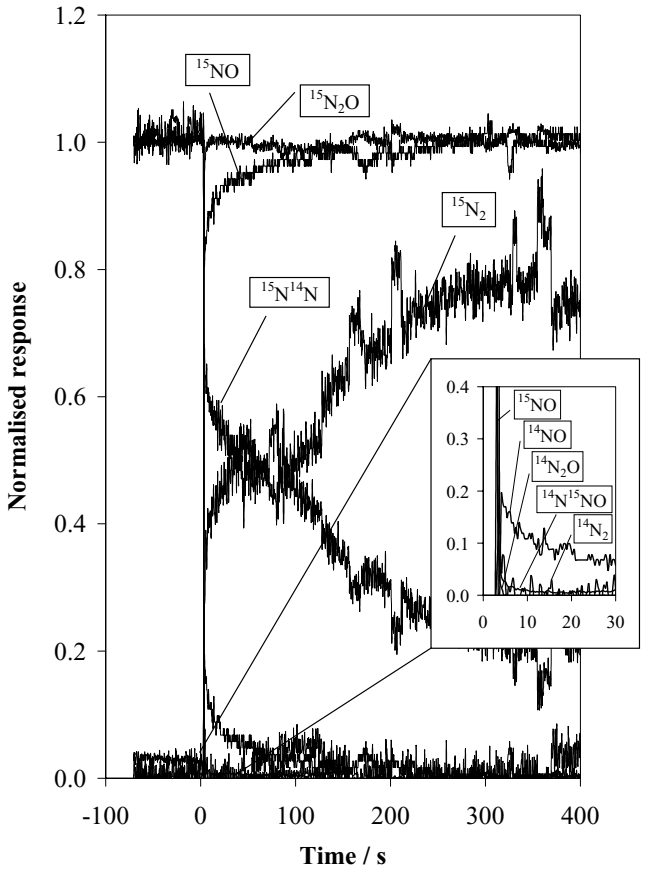

FIG. 12. Concentration profiles as a function of time after a SSITK switch of ^{15}NO for ^{14}NO for a Pt/46Mo/0.27Na/SiO_2 catalyst. Switch from (0.76% ^{14}NO/Ar/1.08% H_2/6% O_2) to (0.76% ^{15}NO/He/1.08% H_2/6% O_2) at 105°C for 100 mg of catalyst at a total gas flow rate of 100 cm^3 min^{-1}.

In particular, the rise in the concentration of N_2O and N_2 is much slower in the case of the promoted catalyst, indicating that the species responsible for the enhanced production of N_2 when the H_2 supply was cut off may also be formed slowly when the H_2 supply is restored. Thus, it seems that while H_2 is consumed to make H_2O at similar rates in both catalysts, some of the H_2 on the Pt surface is not immediately available to produce N_2. We discuss possible reasons for this behaviour later.

DISCUSSION

To facilitate the discussion of the results we first summarise the main observations.

- Addition of small amounts of Na to a Pt catalyst enhances significantly the activity in the NO/H_2 reaction under lean-burn conditions, but higher amounts of Na inhibit the reaction.
- Addition of Na at any level has no promoting effect on the N_2/N_2O selectivity at lower temperatures but lowers the selectivity to N_2 at higher temperatures.
- Addition of Mo oxide as a second promoter significantly increases the NO conversion with peak values now in excess of 90%.
- Mo oxide promotes the selectivity to N_2 relative to N_2O across the whole temperature range of the experiments.
- For the unpromoted Pt catalyst, SSITK experiments show that $^{14}N_2O$ and $^{14}N^{15}NO$ are only formed when gaseous ^{14}NO is present whereas $^{14}N^{15}N$ and $^{14}N_2$ continue to be formed for at least 1500 s after the supply of ^{14}NO is cut off.
- Addition of Na delays the desorption of ^{14}NO and causes a parallel increase in the decay time for the labelled N_2O products.
- Addition of Mo oxide causes the labelled N_2O profiles to decay faster than the ^{14}NO profile and also significantly slows down the labelled N_2 profiles so that the maximum in the $^{14}N^{15}N$ curve occurs later than before and does not decay to zero even after 1500 s.
- With the silica-supported catalyst under rich conditions, the $^{14}N_2$ profile decays very rapidly to zero after the supply of ^{14}NO is cut off; the $^{14}N^{15}N$ mixed isotopic product

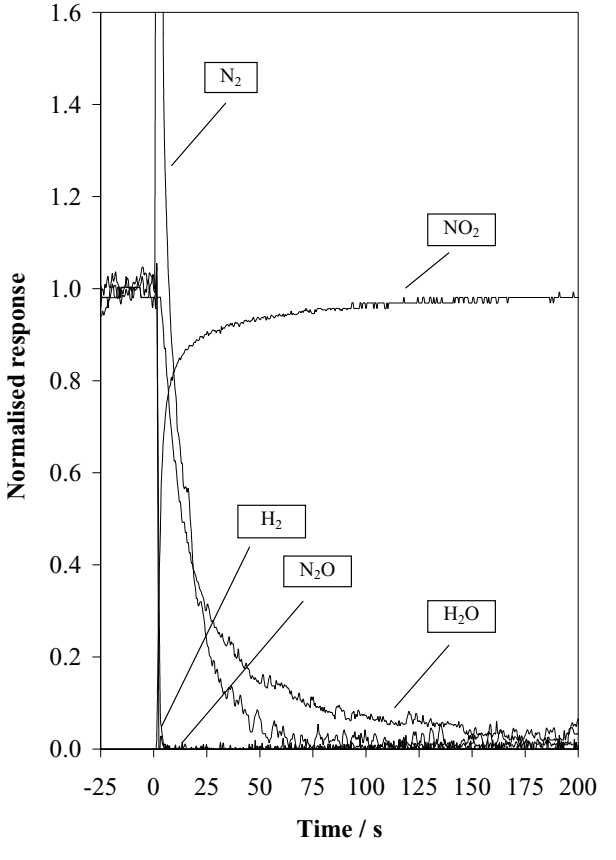

FIG. 13. Concentration profiles as a function of time after switching off the H_2 supply for a Pt/SiO_2 catalyst. Switch from (0.5% NO/12.9% H_2/13.3% O_2) to (0.5% NO/Ar/13.3% O_2) at 110°C for 100 mg of catalyst at a total flow of 180 cm^3 min^{-1}.

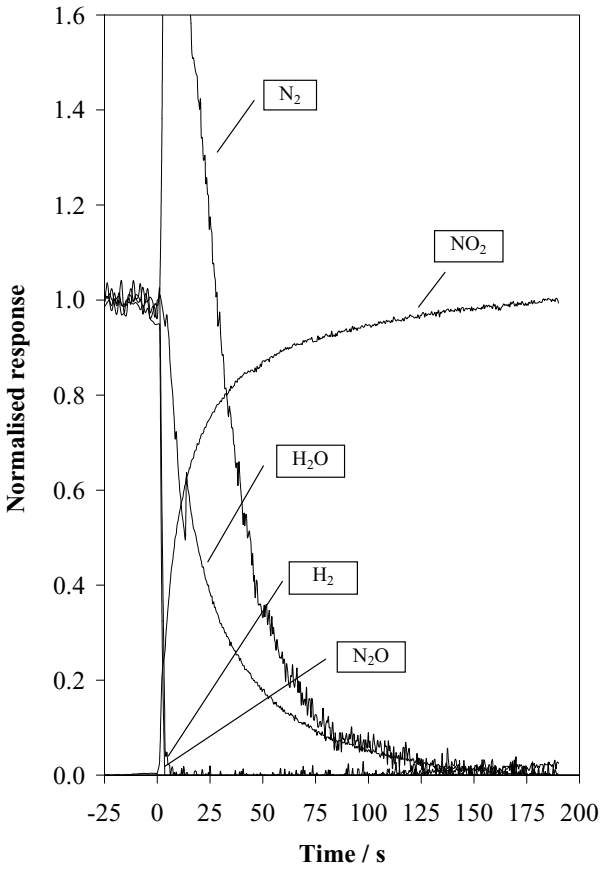

FIG. 14. Concentration profiles as a function of time after switching off the H_2 supply for a Pt/46Mo/0.27Na/SiO_2 catalyst. Switch from (0.5% NO/12.9% H_2/13.3% O_2) to (0.5% NO/Ar/13.3% O_2) at 110°C for 100 mg of catalyst at a total flow of 180 cm^3 min^{-1}.

also decays more rapidly as compared with the alumina-supported catalyst.

- Addition of Mo oxide produces no significant change in the $^{14}N_2$ profile but the $^{14}N^{15}N$ profile now decays very slowly indeed.
- For the silica-supported catalyst under lean conditions, the decay of the $^{14}N^{15}N$ profile is much faster in the presence of oxygen, but for the Mo-promoted catalyst the $^{14}N^{15}N$ decays more slowly. Note also that for the Mo-promoted catalyst the $^{14}N^{15}NO$ decays very rapidly.
- In non-steady-state experiments the formation of N_2O immediately stops when the H_2 supply is cut off whereas there is a transient increase in N_2 formation. For the Mo-promoted catalyst, the N_2O behaves similarly but there is now a very large production of N_2 even though there is no gas-phase reductant present to react with the NO.
- When the H_2 supply is reconnected, the concentrations of N_2O and N_2 recover much more slowly on the Mo-promoted catalyst.

Under stoichiometric conditions, Marina *et al.* (37) have reported that the addition of sodium promotes both the reduction of NO and the selectivity to N_2 rather than to N_2O for a Pt film deposited on Al_2O_3. The optimum coverage of the Pt surface with sodium was 0.06. In our experiments under lean conditions we find that while small amounts of sodium enhance the activity, larger loadings lead to poisoning of the Pt catalyst. Moreover, sodium has no promoting effect on N_2 formation at low temperatures and actually reduces the selectivity at higher temperatures. Clearly under oxidising conditions the dissociation of NO is not enhanced to the same extent as was found by Marina *et al.* under stoichiometric conditions. This is consistent with the fact that a partially oxidised Pt surface will contain fewer suitable sites (for example, two adjacent free Pt atoms) where dissociative adsorption of NO can occur.

The effect of sodium on a reduced Pt surface is thought to be to enhance the adsorption and dissociation of NO so that the formation of N_2O via a N(ads) + NO(ads) reaction is inhibited (37–44). However, while the role of sodium is quite possibly to facilitate NO dissociation, this particular mechanistic step is not consistent with our earlier work on the NO/H_2 reaction (33, 34, 55) nor with many of the new

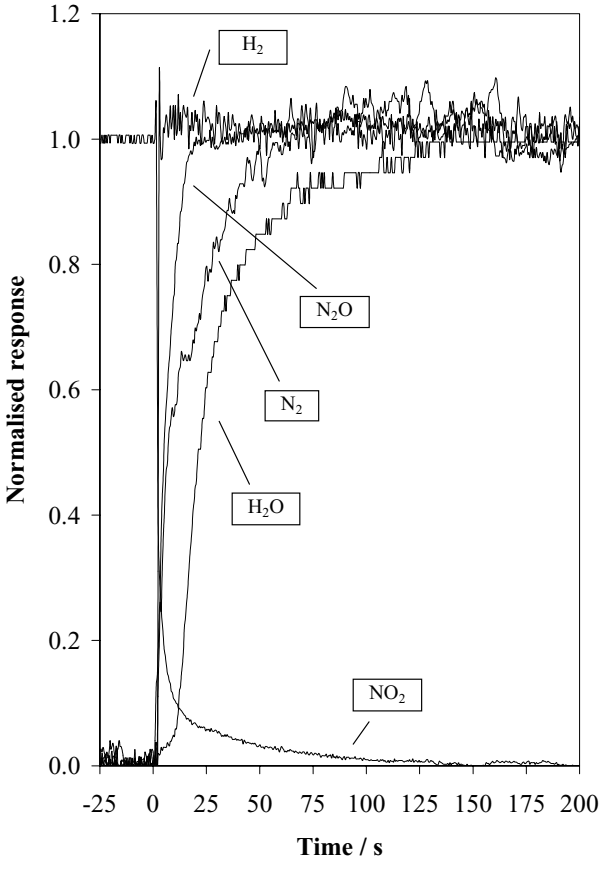

FIG. 15. Concentration profiles as a function of time after switching on the H_2 supply for a Pt/SiO_2 catalyst. Switch from (0.5% NO/Ar/13.3% O_2) to (0.5% NO/12.9% H_2/13.3% O_2) at 110°C for 100 mg of catalyst at a total flow of 180 cm^3 min^{-1}.

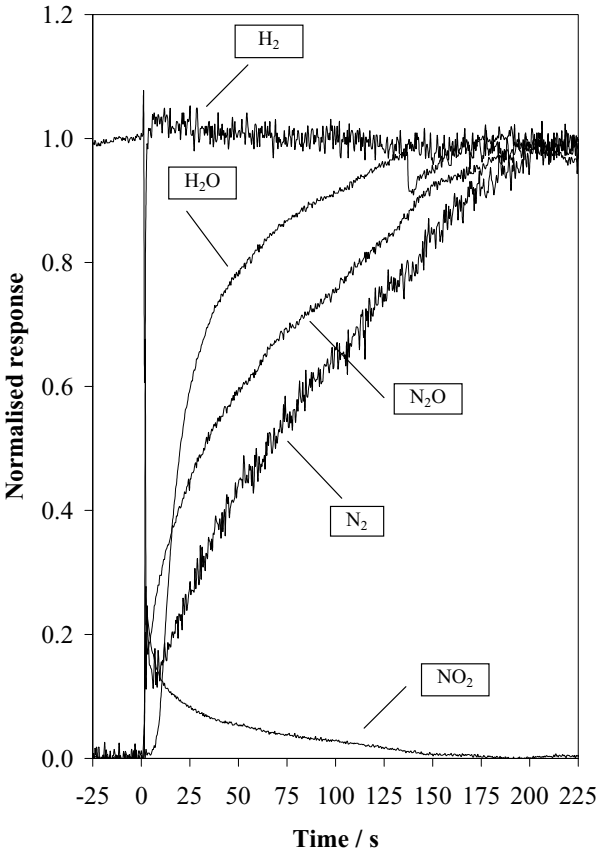

FIG. 16. Concentration profiles as a function of time after switching on the H_2 supply for a Pt/46Mo/0.27Na/SiO_2 catalyst. Switch from (0.5% NO/Ar/13.3% O_2) to (0.5% NO/12.9% H_2/13.3% O_2) at 110°C for 100 mg of catalyst at a total flow of 180 cm^3 min^{-1}.

results presented in the present work. For example, we see in Fig. 5 that the $^{14}N^{15}NO$ profile decays and the $^{15}N_2O$ rises at essentially the same rate as the ^{14}NO and ^{15}NO profiles fall and rise, respectively. This shows that the formation of N_2O requires the presence of gas-phase NO, which is not too surprising. However, the fact that the N_2O profiles change so rapidly also indicates that this product cannot be formed from N(ads) and NO(ads) in significant amounts since there is a large reservoir of N(ads) on the surface, as demonstrated by the long delay in the various isotopically labelled N_2 profiles.

Previously we proposed (33, 34) that N_2O is formed at these lower temperatures through the following reaction:

$$NO(ads) + NO(ads) = N_2O + O(ads).$$

The present SSITK experiments are consistent with this model.

The N_2 profiles for the alumina- and silica-supported Pt show significant differences. With the alumina-supported catalyst the $^{14}N_2$ profile takes over 1000 s to decay whereas with the silica-supported catalyst the $^{14}N_2$ decays extremely rapidly. We attribute this to the fact that alumina can store NO_x, possibly as a nitrite or nitrate, but this does not occur with silica. Therefore, the slow decay in the $^{14}N_2$ profile in the case of alumina could indicate that NO_x species adsorbed on the alumina can reverse spillover back to the Pt to combine with ^{15}N(ads) atoms, or to dissociate and combine with ^{15}NO(ads). We propose this N(ads) + NO(ads) route to N_2 based on our earlier work (33, 34) and also on the fact that with the silica-supported catalyst there is no formation of $^{14}N_2$ as soon as the ^{14}NO is switched off even though there is a large reservoir of ^{14}N that can subsequently form $^{14}N^{15}N$.

Figure 11 also confirms for the silica-supported catalyst that under lean conditions the formation of $^{14}N_2$ does not occur in the absence of gaseous ^{14}NO. Note also (see Fig. 13) that in non-steady-state experiments N_2O formation ceases immediately when the reductant supply (hydrogen) is cut off. This suggests either that N_2O formation is blocked when the surface becomes over oxidised even though N_2 formation can still proceed, or that NO(ads) molecules simply scavenge N(ads) atoms faster than they can couple with other NO(ads) molecules to produce N_2O. The fact that NO_2 is observed soon after the H_2 is cut off is consistent with a competition for NO, either by O(ads) to give NO_2, or by N(ads) to give N_2, so that the NO(ads) + NO(ads) → N_2O + O(ads) reaction is inhibited, as observed in Fig. 13.

We now consider the role of Mo oxide as a promoter of the NO reduction reaction. Mo oxide has the following effects: enhances N_2 selectivity; accelerates the decay of the N_2O profile relative to that of NO; slows down the decay of the N_2 profiles for both alumina- and silica-supported Pt; under lean conditions greatly reduces the rate of decay of the $^{14}N^{15}N$ profile as compared to the unpromoted catalyst; significantly increases the concentration of adsorbed species leading to N_2 but has no effect on the concentration of adsorbed species leading to N_2O (see Table 2); in non-steady-state experiments allows the generation of a very large N_2 peak when the H_2 is cut off and the recovery of the N_2 (and N_2O) peaks when the H_2 is restored is very slow.

The only related work in the literature is that of Tanaka *et al.* (58), where for the reduction of NO by C_3H_6 they report that NO is selectively reduced in the presence of O_2 and attribute this to a lower affinity of Pt for oxygen when the Pt is modified by Mo. In our work it seems that the Mo oxide has a much more significant role and, in addition to any small effect on the electronic properties of Pt, may also be *directly* involved in the conversion of NO to N_2. Thus, it seems unlikely that electronic modifications of the Pt could account for the extremely large changes in the quantity of adsorbed species leading to the formation of N_2, for example, as shown in Table 2. We suggest that the Mo oxide also plays a direct role. Analysis of the results of the switching experiments (see, for example, Figs. 13 and 14) shows that in the absence of H_2 there is a temporary, but

very large, production of N_2 from NO in a Mo-containing catalyst. Clearly, this catalyst has stored on its surface a substantial amount of a species that can *reduce* NO. In our experiments this has to be a hydrogen-containing species. H(ads) itself is ruled out because even if this was present under oxidising conditions, it would only be adsorbed on the Pt and there is no reason why the amount of H(ads) should be affected by the addition of Mo oxide (see the relevant chemisorption results in Table 1).

A more probable explanation is that the Mo oxide captures a reduced form of nitrogen that may be either formed on the Mo oxide or spillover from the Pt to adjacent Mo oxide sites. NH_3, or at least an NH_x-type species, seems the most likely candidate. Indeed ammonium molybdate is a well-known compound and so adsorption of NH_3 on the surface of Mo oxide, leading even to some bulk formation if the kinetics are satisfactory, seems entirely plausible. Preliminary FTIR experiments have failed to confirm the presence of NH_x-type species. However, in a separate study (62) the formation and capture of NH_3 has been observed with ceria–zirconia-supported Pt catalysts in the NO/H_2 reaction and a similar process may operate with the Mo oxide-promoted catalyst.

CONCLUSIONS

It has been shown that for the reduction of NO by H_2 under lean conditions at temperatures representative of automotive "cold-start" conditions the activity and nitrogen selectivity of platinum-based catalysts can be significantly increased by addition of MoO_3 and Na_2O. Addition of the latter was revealed to increase NO conversion activity at low loading; however, the catalyst was poisoned at increased loadings. Moreover, the nitrogen selectivity remained unaffected at low temperatures for all loadings studied, with adverse effects becoming evident as the temperature was raised. The MoO_3 promoter significantly increased both the catalyst activity and selectivity at all loadings. Isotopic switching experiments and subsequent SSITK analysis showed that modification with MoO_3 induced substantial increases in the concentration of surface species leading to N_2 product. Moreover, in non-steady-state transient experiments when H_2 was removed from the feed it was shown that N_2 could be produced for a significantly longer time period over the modified catalyst in the absence of any gas-phase reductant. These observations were consistent with the "storage" of a reduced nitrogen species on the MoO_3.

ACKNOWLEDGMENTS

We are grateful to the EPSRC for a postgraduate studentship for MDC. Also, we are thankful for the assistance of S. T. Daniells.

REFERENCES

1. Chiron, M., *Stud. Surf. Sci. Catal.* **30**, 1 (1987).
2. Armor, J. N., *Appl. Catal. B* **1**, 221 (1992).
3. De Kermikri, I., *Recherche* **279**, 884 (1995).
4. Adams, K. M., Cavataio, J. V., and Hammerle, R. H., *Appl. Catal. B* **10**, 157 (1996).
5. Bond, G. C., "Heterogeneous Catalysis," 2nd ed. Oxford University Press, Oxford, UK, 1987.
6. Fritz, A., and Pitchon, V., *Appl. Catal. B* **13**, 1 (1997).
7. Hu, Z., Allen, F. M., Wan, C. Z., Heck, R. M., Steger, J. J., Lakis, R. E., and Lyman, C. E., *J. Catal.* **174**, 13 (1998).
8. Harrison, B., Searles, R. A., and Wilkins, A. J. J., *in* "Car Exhaust Pollution Control: Lean-Burn Engines & the Continuing Requirement for Platinum-Containing Autocatalysts" (J. W. S. Longhurst, Ed.), p. 327. British Library, Technical Communications, 1989.
9. Gutierrez, L., Boix, A., and Petunchi, J. O., *J. Catal.* **179**, 179 (1998).
10. Ribotta, A., Lezcano, M., Kurgansky, M., Miro, E., Lombardo, E., Petunchi, J., Moreaux, C., and Dereppe, J. M., *Catal. Lett.* **49**, 77 (1997).
11. Cowan, A. D., Cant, N. W., Haynes, B. S., and Nelson, P. F., *J. Catal.* **176**, 329 (1998).
12. Lombardo, E. A., Sill, G. A., d'Itri, J. L., and Hall, W. K., *J. Catal.* **173**, 440 (1998).
13. Ohtsuka, H., and Tabata, T., *Appl. Catal. B* **21**, 133 (1999).
14. Sullivan, J. A., and Cunningham, J., *Appl. Catal. B* **15**, 275 (1998).
15. Long, R., and Yang, R. T., *Catal. Lett.* **52**, 91 (1998).
16. Okazaki, N., Shiina, Y., Itoh, H., Tada, A., and Iwamoto, M., *Catal. Lett.* **49**, 169 (1997).
17. Halasz, I., and Brenner, A., *Catal. Lett.* **51**, 195 (1998).
18. Burch, R., and Watling, T. C., *J. Catal.* **169**, 45 (1997).
19. Burch, R., Sullivan, J. A., and Watling, T. C., *Catal. Today* **42**, 13 (1998).
20. Burch, R., and Watling, T. C., *Catal. Lett.* **37**, 51 (1996).
21. Hayes, N. W., Joyner, R. W., and Shpiro, E. S., *Appl. Catal. B* **8**, 343 (1996).
22. Kameoka, S., Chafik, T., Ukisu, Y., and Miyadera, T., *Catal. Lett.* **55**, 211 (1998).
23. Delahay, G., Ensuque, E., Coq, B., and Figueras, F., *J. Catal.* **175**, 7 (1998).
24. Shimizu, K.-I., Satsuma, A., and Hattori, T., *Appl. Catal. B* **25**, 239 (2000).
25. Burch, R., Fornasiero, P., and Southward, B. W. L., *J. Catal.* **182**, 234 (1999).
26. Burch, R., Fornasiero, P., and Southward, B. W. L., *Chem. Commun.* 739 (1998).
27. Burch, R., Fornasiero, P., and Southward, B. W. L., *Chem. Commun.* 625 (1998).
28. Ertl, G., Knozinger, H., and Weitkamp, J., Ed., "Environmental Catalysis." Wiley-VCH, New York, 1999.
29. Taylor, K. C., and Klimisch, R. L., *J. Catal.* **30**, 478 (1973).
30. Yao, H. C., Yu Yao, Y.-F., and Otto, K., *J. Catal.* **56**, 21 (1979).
31. Otto, K., and Yao, H. C., *J. Catal.* **66**, 229 (1980).
32. Sharpe, R. G., and Bowker, M., *Surf. Sci.* **360**, 21 (1996).
33. Burch, R., Shestov, A. A., and Sullivan, J. A., *J. Catal.* **186**, 353 (1999).
34. Shestov, A. A., Burch, R., and Sullivan, J. A., *J. Catal.* **186**, 362 (1999).
35. Kobylinski, T. P., and Taylor, B. W., *J. Catal.* **33**, 376 (1974).
36. Harkness, I. R., and Lambert, R. M., *J. Chem. Soc. Faraday Trans.* **93** (7), 1425 (1997).
37. Marina, O. A., Yentekakis, I. V., Vayenas, C. G., Palermo, A., and Lambert, R. M., *J. Catal.* **166**, 218 (1997).
38. Palermo, A., Lambert, R. M., Harkness, I. R., Yentekakis, I. V., Mar'ina, O., and Vayenas, C. G., *J. Catal.* **161**, 471 (1996).
39. Yentekakis, I. V., Konsolakis, M., Lambert, R. M., Macleod, N., and Nalbantian, L., *Appl. Catal. B* **22**, 123 (1999).
40. Yentekakis, I. V., Palermo, A., Filkin, N. C., Tikhov, M. S., and Lambert, R. M., *J. Phys. Chem. B* **101**, 3759 (1997).

41. Macleod, N., Isaac, J., and Lambert, R. M., *J. Catal.* **198**, 128 (2001).
42. Macleod, N., Isaac, J., and Lambert, R. M., *Appl. Catal. B* **33**, 335 (2001).
43. Williams, F. J., Tikhov, M. S., Palermo, A., Macleod, N., and Lambert, R. M., *J. Phys. Chem. B* **105**, 2800 (2001).
44. Williams, F. J., Palermo, A., Tikhov, M. S., and Lambert, R. M., *Surf. Sci.* **482–485**, 177 (2001).
45. Yentekakis, I. V., Konsolakis, M., Lambert, R. M., Palermo, A., and Tikhov, M., *Solid State Ionics* **136**, 783 (2000).
46. Lambert, R. M., Palermo, A., Williams, F. J., and Tikhov, M. S., *Solid State Ionics* **136**, 677 (2000).
47. Williams, F. J., Aldao, C. M., Palermo, A., and Lambert, R. M., *Surf. Sci.* **412/413**, 174 (1998).
48. Yentekakis, I. V., Lambert, R. M., Konsolakis, M., and Kiousis, V., *Appl. Catal. B* **18**, 293 (1998).
49. Halasz, I., Brenner, A., and Shelef, M., *Catal. Lett.* **16**, 311 (1992).
50. Halasz, I., Brenner, A., and Shelef, M., *Appl. Catal. B* **2**, 131 (1993).
51. Halasz, I., Brenner, A., and Shelef, M., *Catal. Lett.* **18**, 289 (1993).
52. Frank, B., Emig, G., and Renken, A., *Appl. Catal. B* **19**, 45 (1998).
53. Costa, C. N., Stathopoulos, V. N., Belessi, V. C., and Efstathiou, A. M., *J. Catal.* **197**, 350 (2001).
54. Ueda, A., Nakao, T., Azuma, M., and Kobayashi, T., *Catal. Today* **45**, 135 (1998).
55. Burch, R., Shestov, A. A., and Sullivan, J. A., *J. Catal.* **188**, 69 (1999).
56. Burch, R., and Coleman, M. D., *Appl. Catal. B* **23**, 115 (1999).
57. Burch, R., and Millington, P. J., *Catal. Today* **26**, 185 (1995).
58. Tanaka, T., Yokota, K., Isomura, N., Doi, H., and Sugiura, M., *Appl. Catal. B* **16**, 199 (1998).
59. Yokota, K., Fukui, M., and Tanaka, T., *Appl. Surf. Sci.* **121/122**, 273 (1997).
60. Tanaka, T., Yokota, K., Doi, H., and Sugiura, M., *Chem. Lett.* 409 (1997).
61. Shannon, S. L., and Goodwin, J. G., Jr., *Chem. Rev.* **95**, 677 (1995).
62. Breen, J. P., Burch, R., and Lingaiah, N., *Catal. Lett.*, in press.